Deep Inelastic ep Scattering at Large Momentum Transfer at HERA

Burkard Reisert for H1 and ZEUS

Theory
- Deep Inelastic Scattering
- Parton Distributions
- NC and CC Cross Sections

Facilities
- HERA Accelerator
- H1 and Zeus Detector

Data
- NC results
- CC results

Conclusions

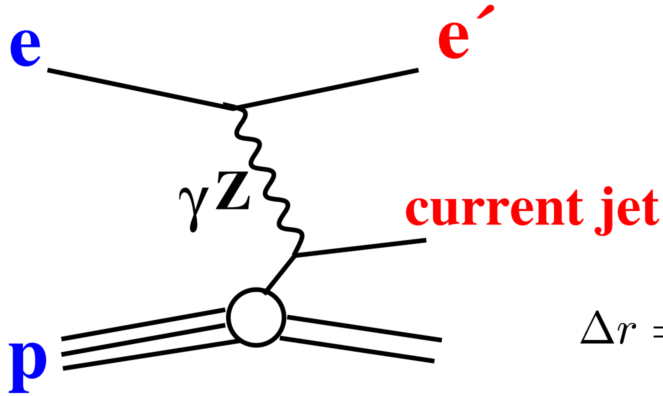

$$\Delta r = \frac{\hbar c}{\sqrt{Q^2}}$$

$$\Rightarrow \Delta r \backsim 10^{-3} fm$$

$$Q^2 \gg M_Z^2, M_W^2$$

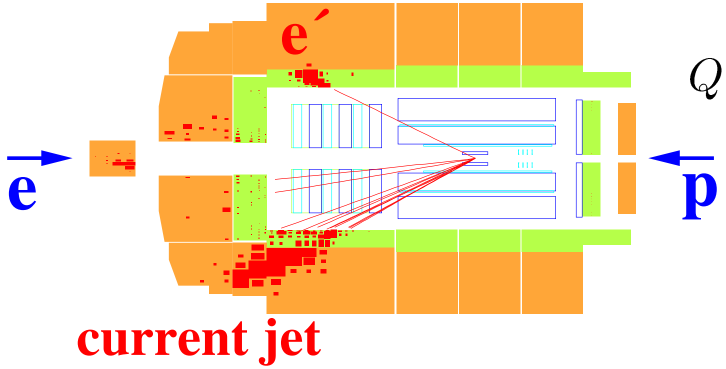

Deep Inelastic Scattering

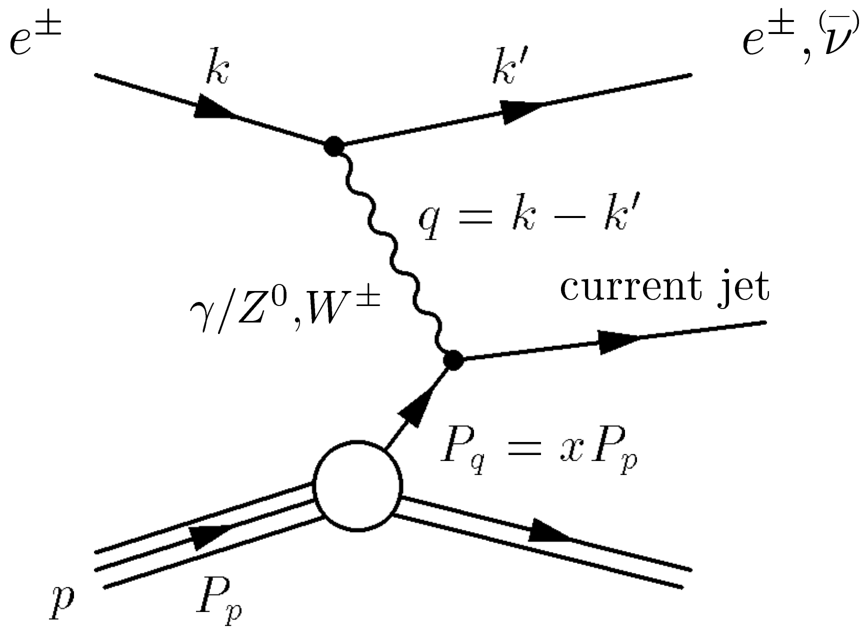

4-momentum transfer

$Q^2 = -q^2 = -(k - k')^2$

parton momentum fraction

$x = Q^2/(2p \cdot q)$

inelasticity

$y = p \cdot q/(p \cdot k)$

center of mass (cms) energy $\sqrt{s}$**:**

$s = (k + p)^2$

at fixed cms energy: $y = Q^2/xs$

neutral current (NC):
γ, Z^0 exchange

charged current (CC):
$W^\pm$ exchange

lepton vertex: pointlike particle,
determined by electroweak Standard Model (SM)
proton vertex: object with structure

quark-parton-modell (QPM):
elastic scattering on pointlike parton (quark);
quark momentum distribution $xq(x)$ inside proton

Partons, F_2, Quantum Chromodynamics (QCD)

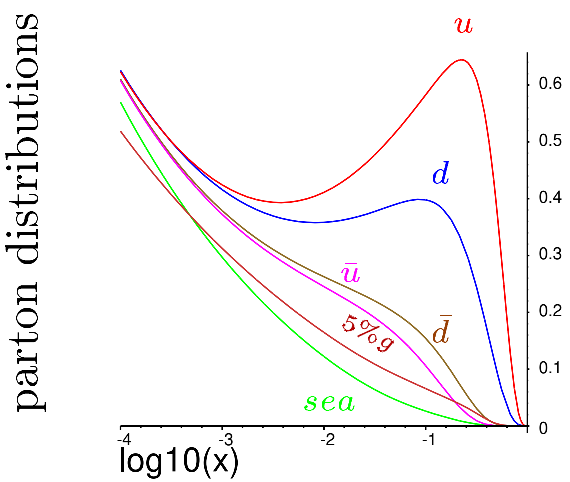

steeply rising sea at low x

dynamics driven by gluon

no theory prediction at fixed $Q_0^2 \Rightarrow$

- measure at fixed (low) Q_0 scale
- calculate QCD evolution in Q^2

popular parametrizations: CTEQ, MRS, GRV, ...

e.g. $q_i(x, Q_0^2) = A_i x^{B_i}(1-x)^{C_i}(1 + xD_i + E_i\sqrt{x})$

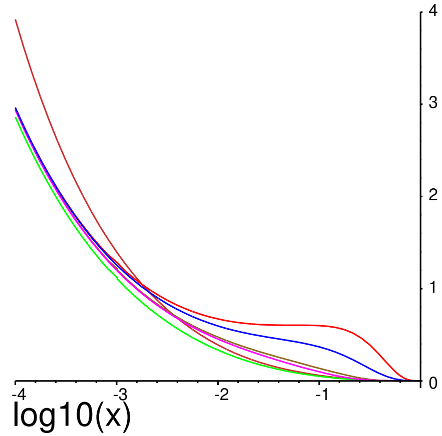

QPM: xq_i do not depend on $Q^2 \rightarrow$ “scaling”

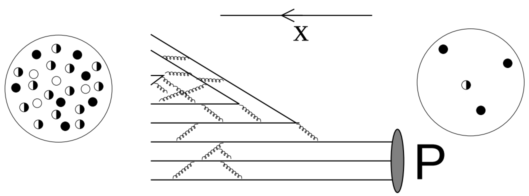

QCD gluon emission $\rightarrow q\bar{q}$ production

$\rightarrow Q^2$ dependence of structure functions

$\rightarrow$ violation of scaling

at large momentum transfer Q^2

more $q\bar{q}$ fluctuations are resolved

populate low x $\leftrightarrow$ depopulate high x

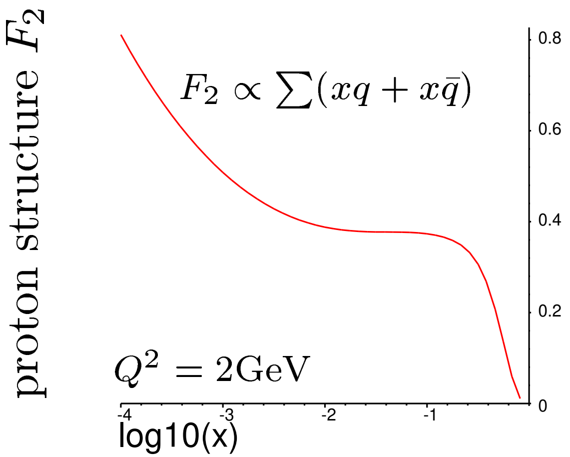

$xq(x, Q^2)$ evolve in Q^2, described by perturbative Quantum ChromoDynamics

pQCD $\rightarrow$ DGLAP evolution equation

(Dokshitzer-Gribov-Lipatov-Altarelli-Parisi)

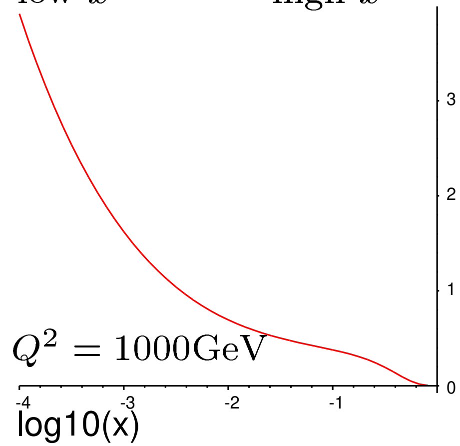

NC Cross Section $ep \to e'X$

neutral current inclusive cross section:

$$\frac{d^2\sigma^{e^\pm p}}{dx\,dQ^2} = \frac{2\pi\alpha^2}{xQ^4}(Y_+F_2(x,Q^2) \mp Y_- xF_3(x,Q^2) - y^2 F_L(x,Q^2)),$$

$$Y_\pm(y) = 1 \pm (1-y)^2$$

proton structure function:

$F_2 = \sum_i A_i(Q^2)\,[xq_i + x\bar{q}_i]$

parity violating structure function:

$F_3 = \quad \sum_i B_i(Q^2)\,[xq_i - x\bar{q}_i]$

longitudinal structure function:

$F_L = F_2 - 2xF_1$ QPM: $F_L = 0$

($F_2 = 2xF_1$ Callan-Gross relation, spin 1/2 partons)

electroweak coefficient functions:

$A_i(Q^2) = e_i^2 - 2e_i v_e v_i P_Z + (v_e^2 + a_e^2)(v_i^2 + a_i^2)P_Z^2$

$B_i(Q^2) = -2e_i a_e a_i P_Z + 4v_e a_e v_i a_i P_Z^2$

with electromagnetic coupling constant e_i

in units of the electron charge $e_e = -1$

weak coupling constants: vector $v_{e,i}$ and axial-vector $a_{e,i}$

and propagator term: $P_Z = \dfrac{1}{4\sin^2\theta_W \cos^2\theta_W}\dfrac{Q^2}{Q^2 + M_Z^2}$

Weinberg angle θ_W: $sin^2\theta_W = 1 - M_W^2/M_Z^2$

CC Cross Section $ep \to \overset{(-)}{\nu} X$

W bosons couple to

left handed fermions

right handed anti fermions

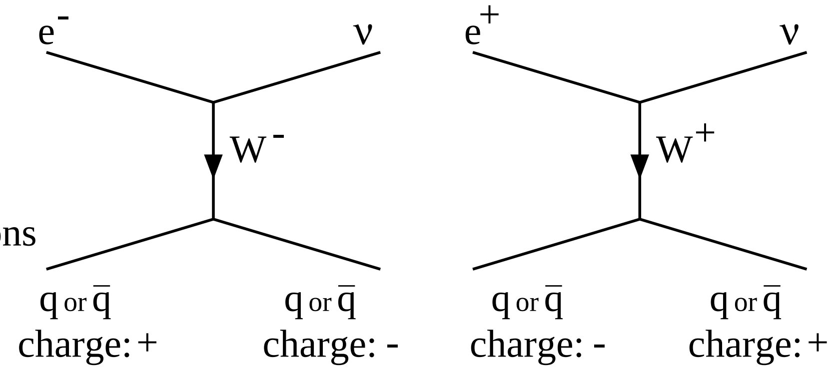

$$\frac{d^2\sigma_{CC}}{dx\,dQ^2} = \frac{G_F^2}{2\pi x}\left(\frac{{M_W}^2}{{M_W}^2+Q^2}\right)^2 \Phi_{CC}(x,Q^2)$$

$$\Phi_{CC}^{e^+p}|_{LO} = (\bar{u}+\bar{c}) + (1-y)^2(d+s)$$

$$\Phi_{CC}^{e^-p}|_{LO} = (u+c) + (1-y)^2(\bar{d}+\bar{s})$$

Helicity Depencence

forward hemisphere

helicity H

J_Z z comp. of
ang. momentum

backward hemisphere

amplitude

θ^* polar angle (cms)
$y=1/2(1+\cos\theta^*)$

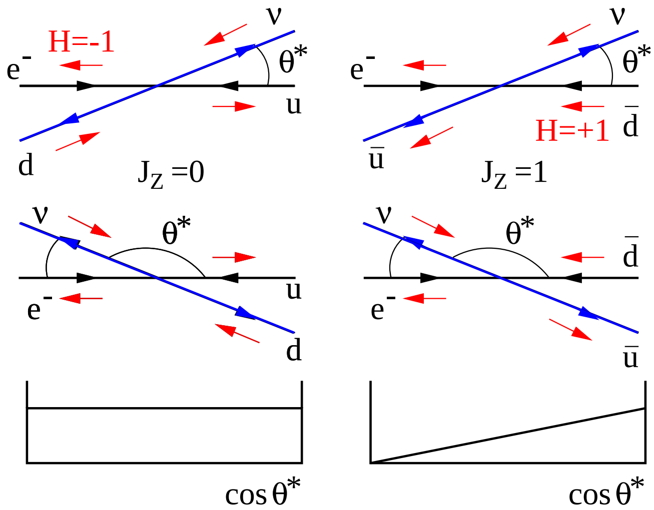

- extract mass of propagator in a spacelike process
  $\longrightarrow$ W mass
- probe valence d and u quarks at large Q^2, large x

HERA Kinematic Plane

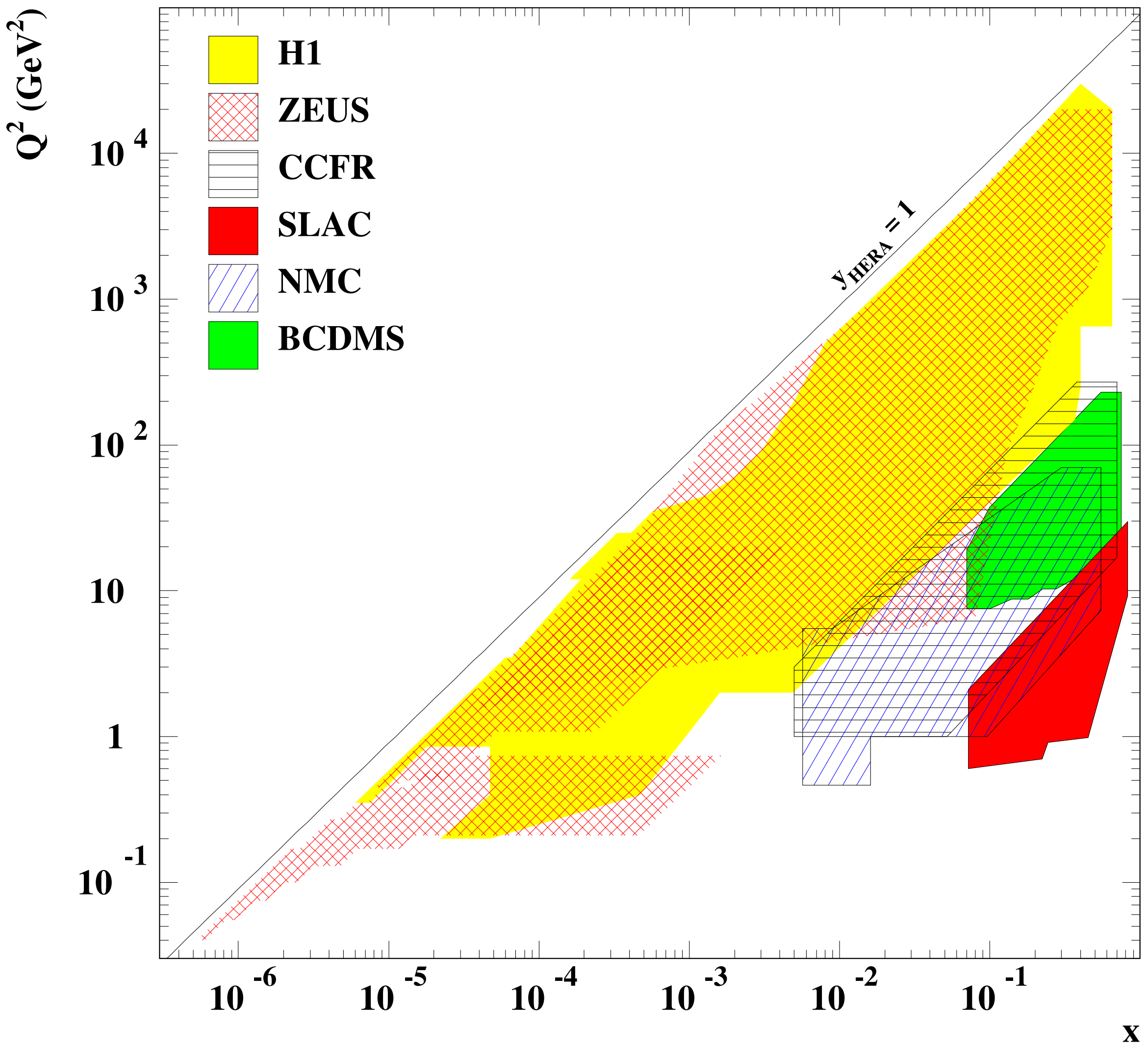

HERA beam energies:

1994-97: $\sqrt{s} = 300$ GeV

e^+ 27.5 GeV, p 820 GeV

1998-99: $\sqrt{s} = 320$ GeV

e^- 27.5 GeV, p 920 GeV

HERA resolves proton structure

– down to small momenta

$x \approx 10^{-6}$

– in wide range of Q^2:

$\mathcal{O}\,0.01 GeV^2 < Q^2 < \mathcal{O}\,10^4 GeV^2$

– at very short distances:

$\approx 10^{-18}$ m

Two colliding beam experiments:

H1 and ZEUS

overlap with fixed target

experiments at $y \approx 0.003$

H1 Detector

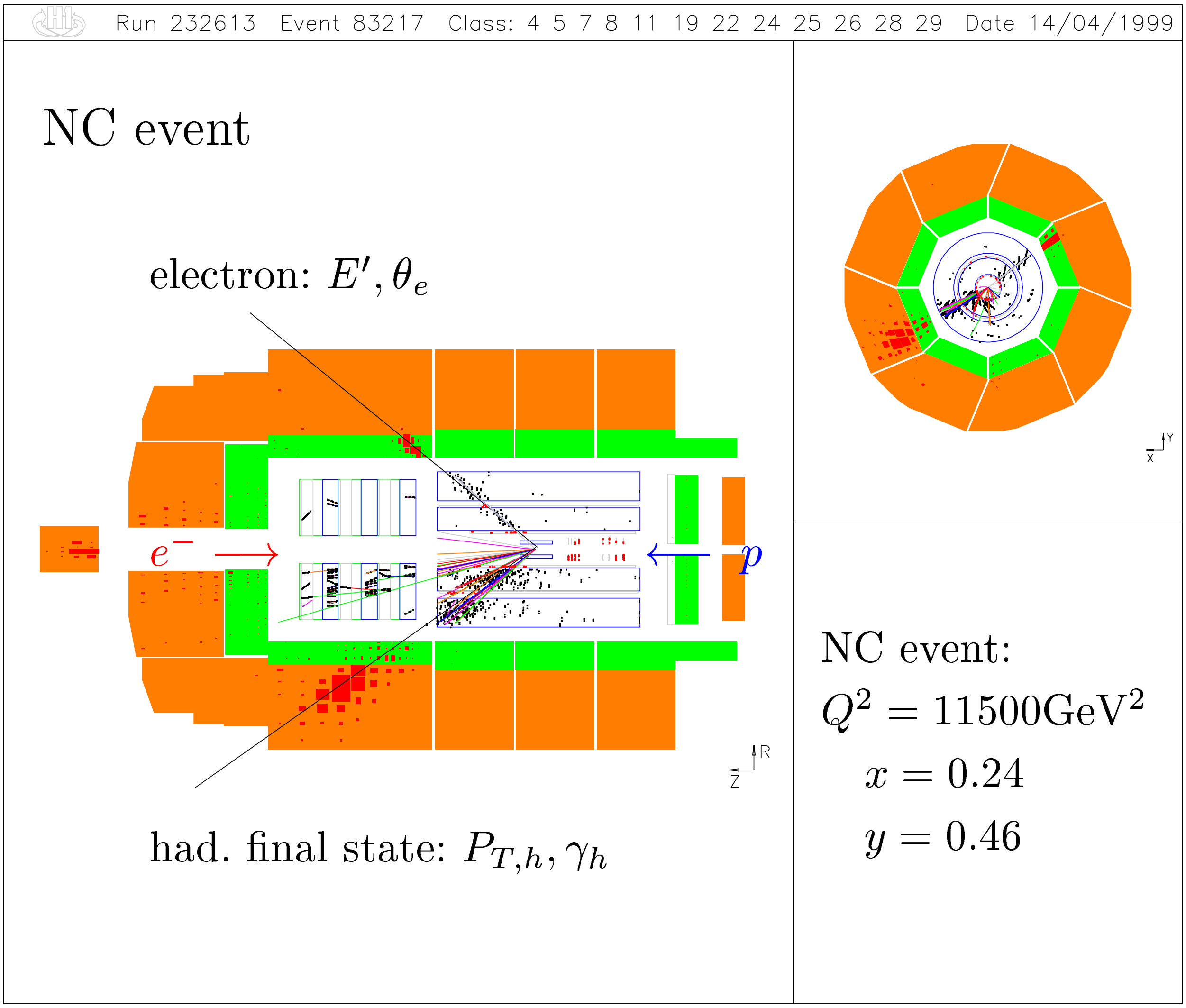

Liquid Argon Calorimeter (LAr):

high granularity – 45000 cells

EM section

$\sigma(E)/E = 12\%/\sqrt{E} \oplus 1\%$

syst. unc.: $1 - 3\%$

$\sigma(\theta_e)$: 3 mrad calorimeter

1 mrad tracker

HAD section

$\sigma(E)/E = 50\%/\sqrt{E} \oplus 1\%$

syst. unc.: $3 - 4\%$

Zeus Detector

CC event: $\nu(\bar{\nu})$ escapes detection

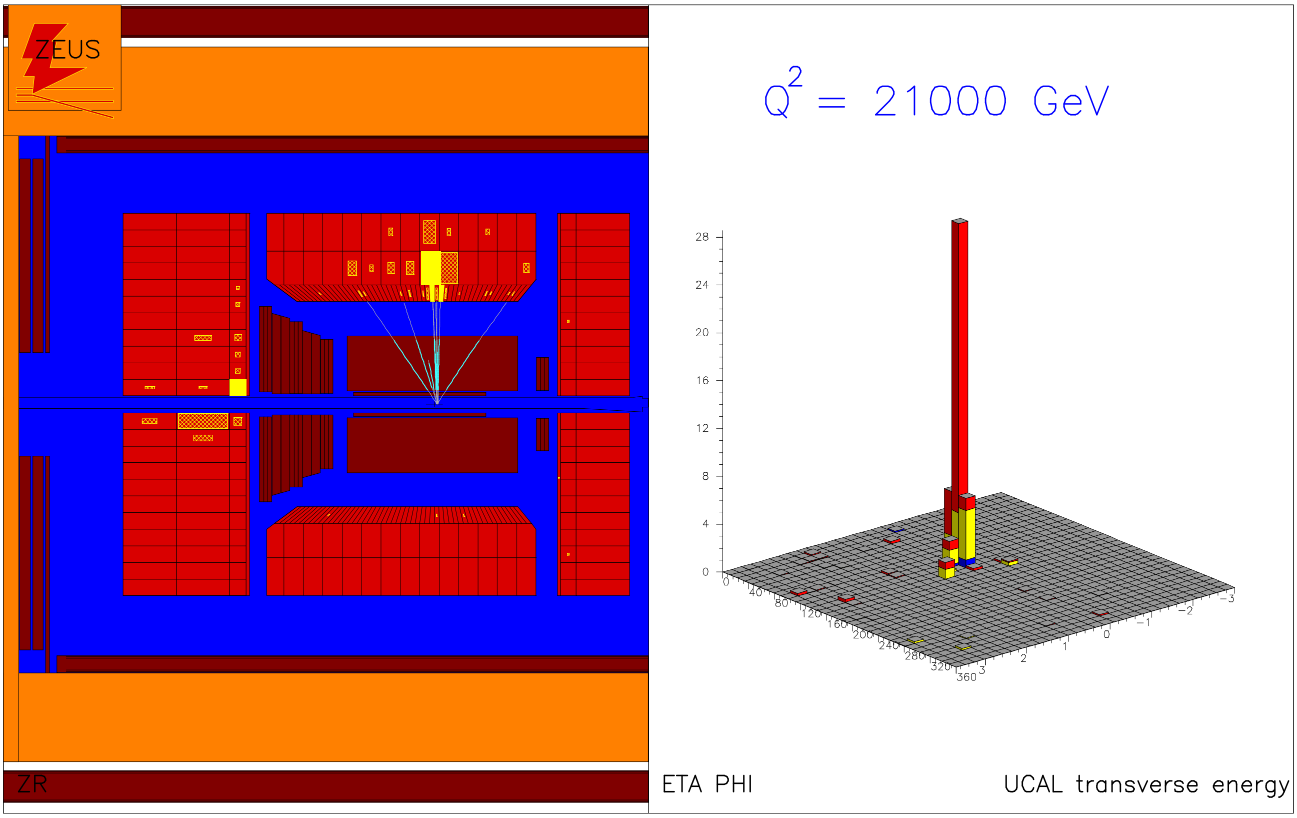

Compensating Uranium Scintillator Calorimeter

6000 cells

$$\sigma(\theta_e) = 2\text{mrad}; \; \frac{\sigma}{\sqrt{E'_e}} = 18\%;$$

$$\frac{\sigma}{\sqrt{E_h}} = 35\% \; \Delta E/E(syst) = 1 - 3\%;$$

Reconstruction of Kinematics

electron/positron: E'_e, θ_e

had. final state: $P_{T,h} = \sqrt{(\sum_i p_{x,i})^2 + (\sum_i p_{y,i})^2}$

$$\tan\frac{\gamma_h}{2} = \frac{\sum_i (Ei - p_{z,i})}{P_{T,h}}$$

summed over hadronic final state

Electron Method (H1): E'_e,θ_e

$Q^2_e = 4E_e E'_e \cos^2\frac{\theta_e}{2}$,

$y_e = 1 - \frac{E'_e}{2E_e}(1 - \cos\theta_e)$, $x_e = Q^2_e / y_e s$

Double Angle Method (ZEUS): θ_e,γ_h

also used in H1 for calibration purposes

$$Q^2_{DA} = \frac{4E_e^2 \sin\gamma_h (1 + \cos\theta_e)}{\sin\gamma_h + \sin\theta_e - \sin(\theta_e + \gamma_h)},$$

$$y_{DA} = \frac{\sin\theta_e (1 - \cos\gamma_h)}{\sin\gamma_h + \sin\theta_e - \sin(\theta_e + \gamma_h)}, \; x_{DA} = Q^2_{DA}/(s y_{DA})$$

Hadron Method (the only possibility for CC)

$$y_h = \frac{\sum_i (Ei - p_{z,i})}{2E_e}, \quad Q^2_h = \frac{P^2_{T,h}}{1 - y_h}, \quad x_h = \frac{Q^2_h}{s y_h}$$

NC Cross Sections: e^+p (published data)

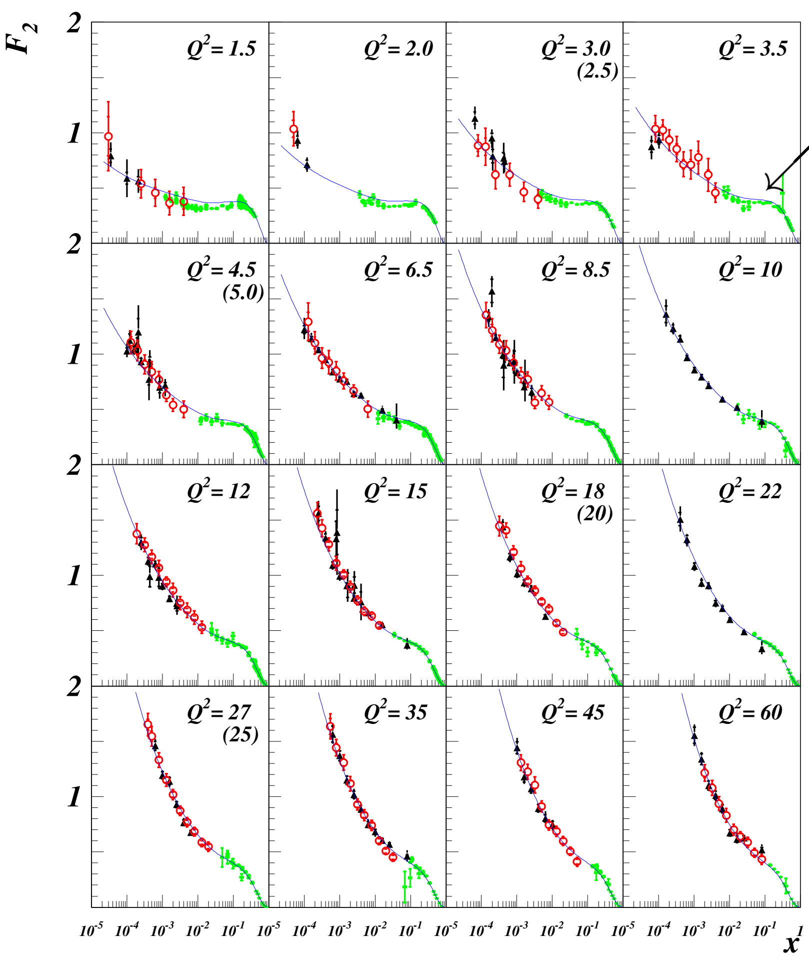

fixed target

H1
ZEUS

in good agreement

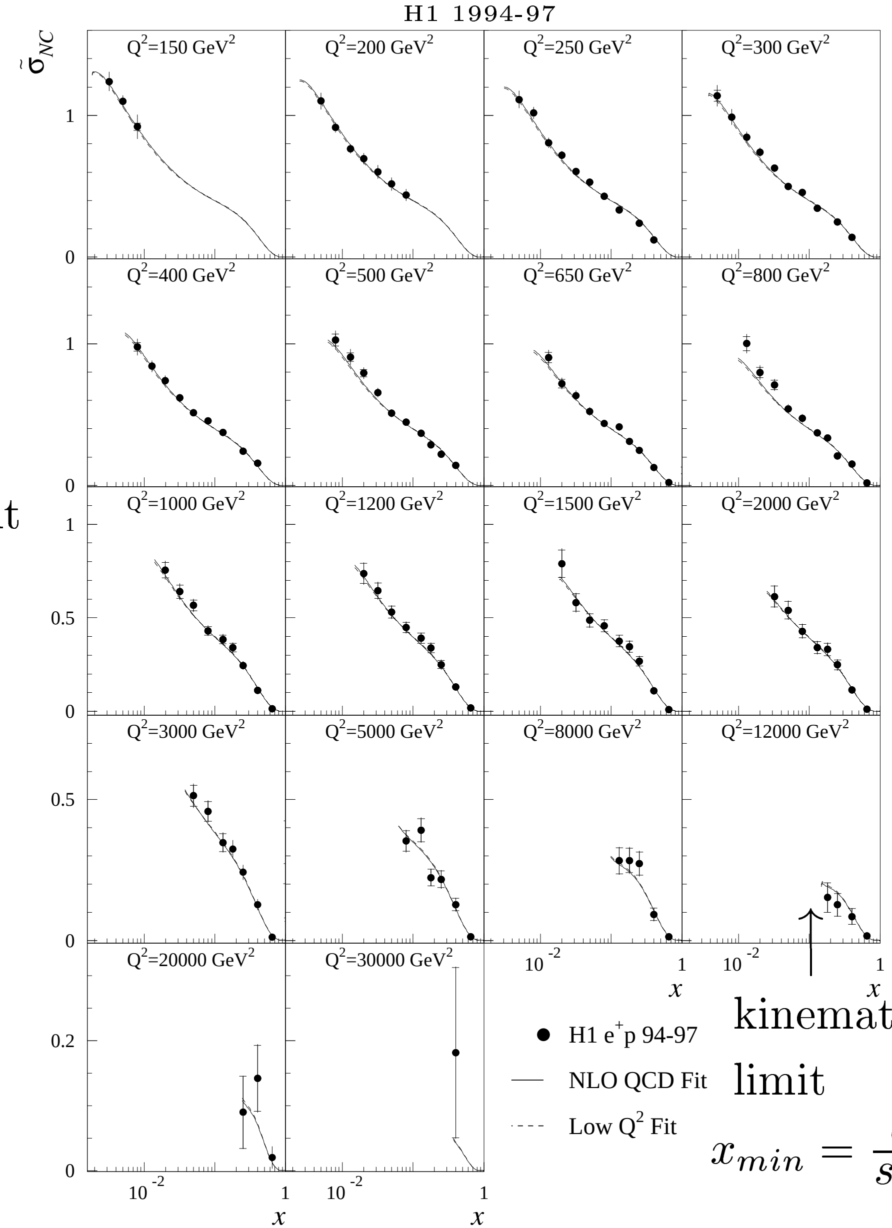

kinematic limit

$$x_{min} = \frac{Q^2}{s \cdot 1}$$

$$\tilde{\sigma}_{NC}(x, Q^2) = \frac{xQ^4}{2\pi\alpha^2} \frac{1}{Y_+} \frac{d^2\sigma_{NC}}{dx\, dQ^2}$$

$$= F_2(x, Q^2)(1 + \underbrace{\Delta F_2 + \Delta F_3}_{\text{electroweak corrections}} + \Delta F_L)$$

Proton Structure Function $F_2(x, Q^2)$

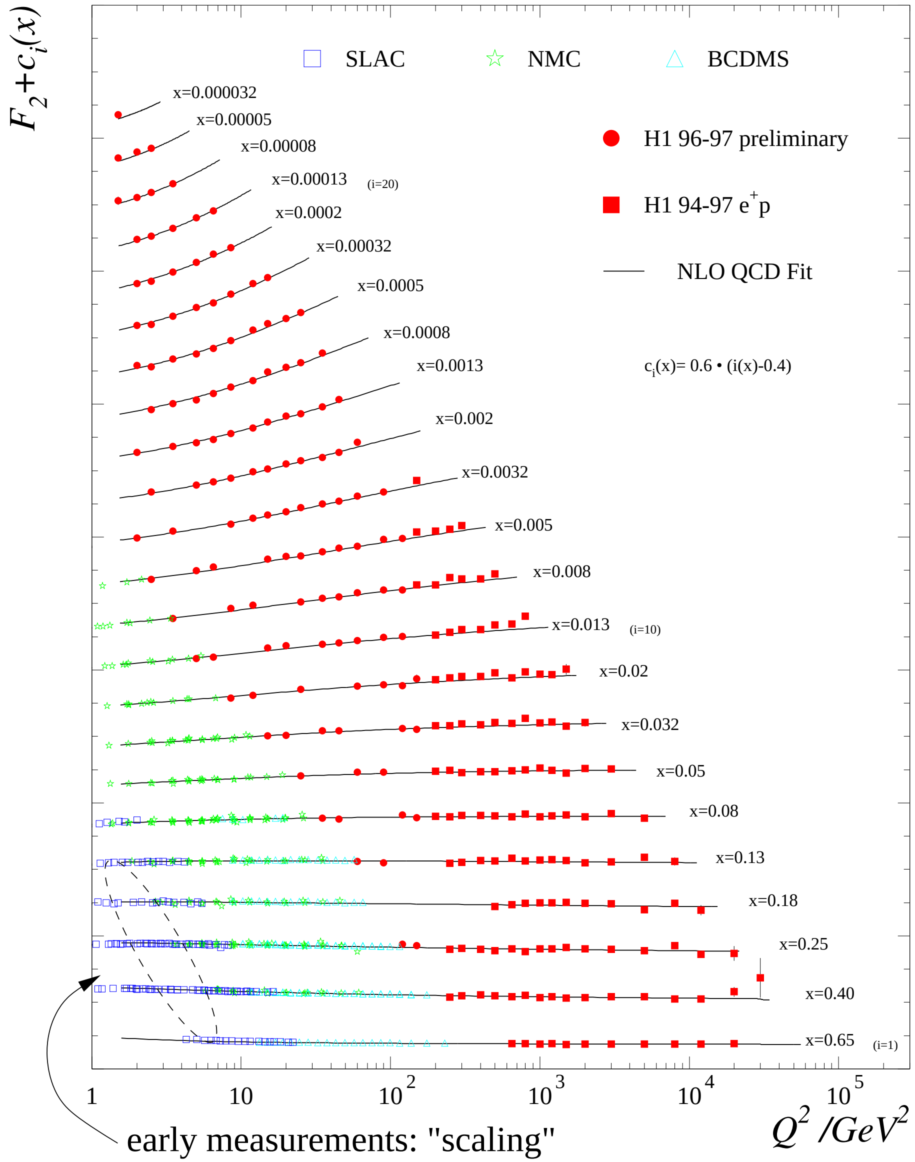

HERA experiments extend range in Q^2 and x by 2 orders of magnitude wrt. fixed target exp.

test of pQCD from $Q^2 \approx 1$ to $Q^2 \approx 30000 GeV^2$ NLO DGLAP evolution works well up to the highest Q^2

observed scaling violations well described by pQCD

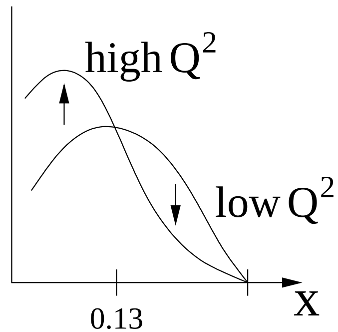

NC Cross Sections $d\sigma^{e^\pm p}/dQ^2$

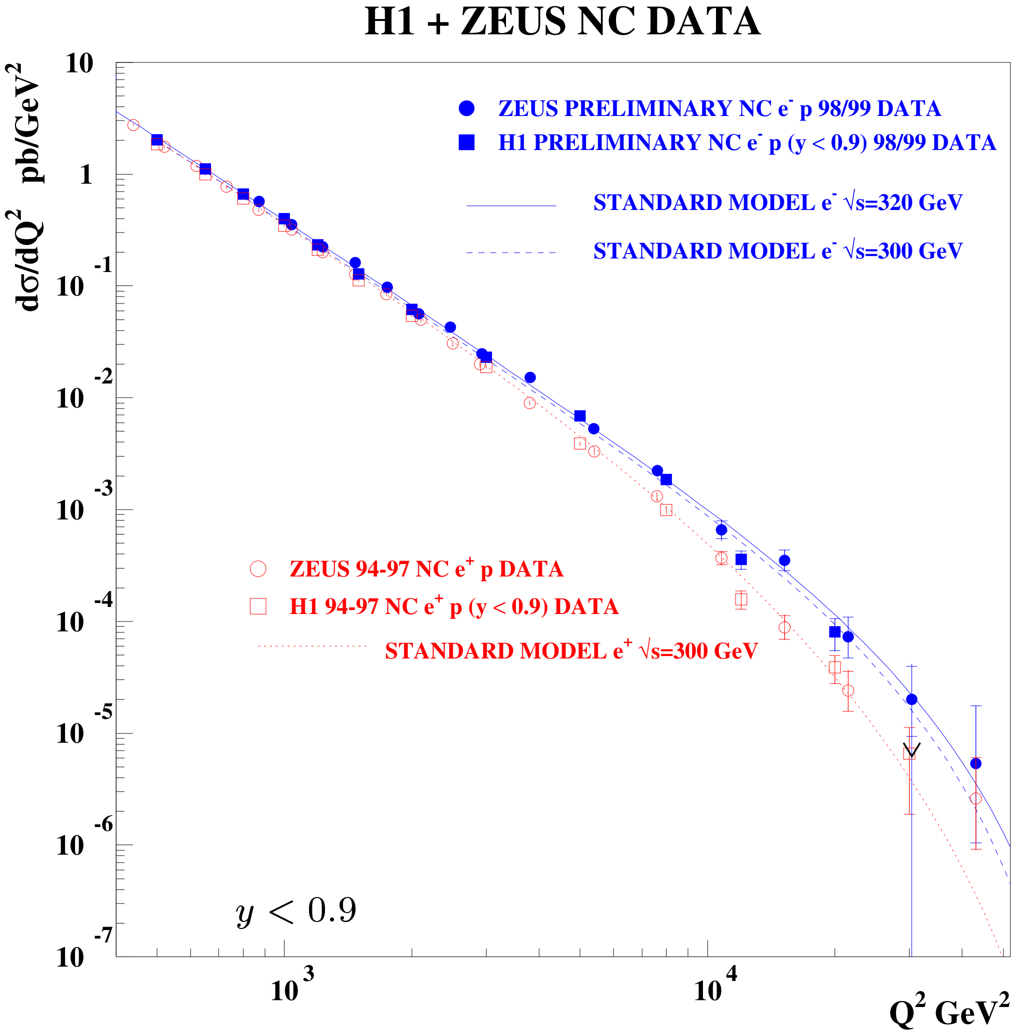

e^+ 1994-97 published
e^- 1998/99 new data

$$\frac{d\sigma}{dQ^2}_{NC} \propto \frac{1}{Q^4} \text{ (at low } Q^2\text{)}$$

difference expected (and seen)
at high Q^2
due to parity violating
electroweak interaction
($e^\pm$: $\mp xF_3$)

NC Cross Section at high x

$e^+p: \ \mathcal{L} = 35pb^{-1}$ $\qquad$ $e^-p: \ \mathcal{L} = 15.3pb^{-1}$

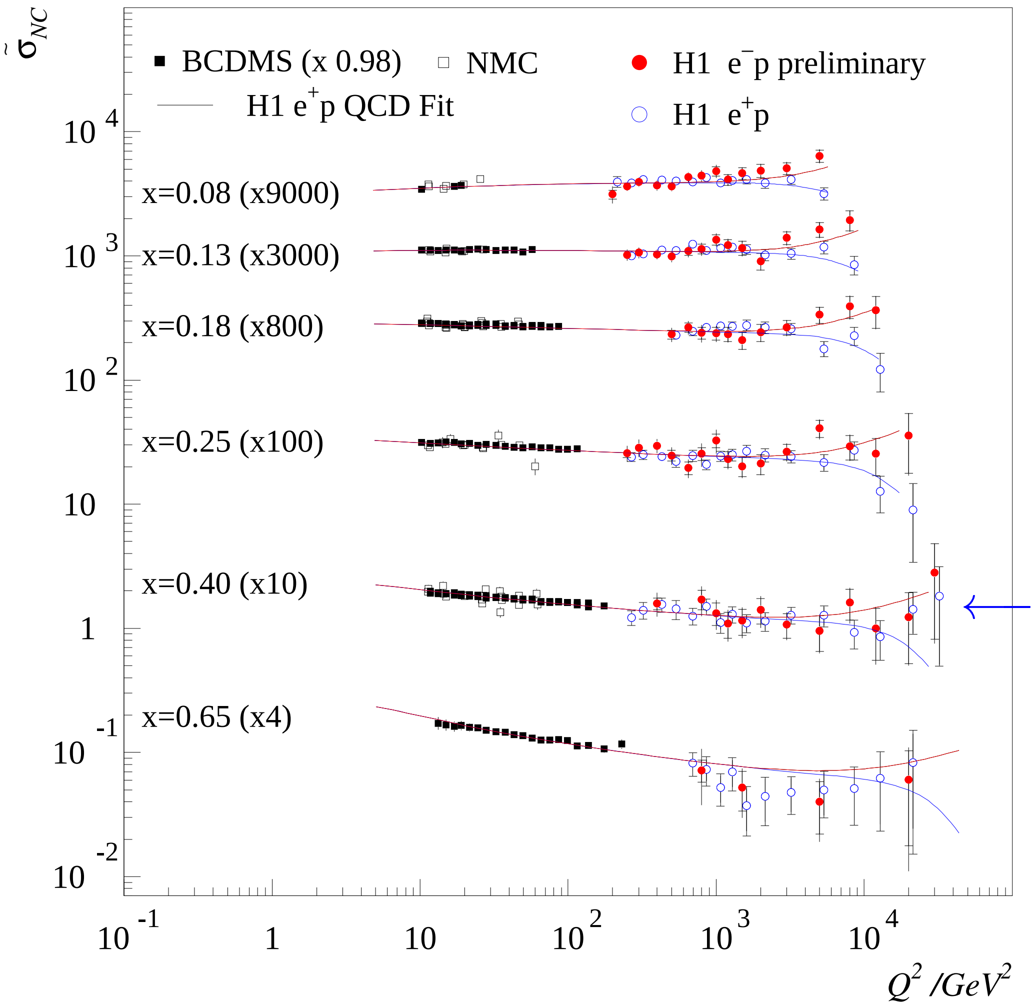

for $Q^2 \gtrsim M_Z^2$ electroweak effects

e^- prediction based on parton distributions extracted from e^+ describe new e^- data

for $x \gtrsim 0.4$ e^+ data slight excess
(two σ effect)
needs more luminosity for clarification

$$\tilde{\sigma}_{NC} = \frac{xQ^4}{2\pi\alpha^2}\frac{1}{Y_+}\frac{d^2\sigma_{NC}}{dx\,dQ^2}$$

NC and CC Cross Section: $d\sigma^{e^{\pm}p}/dQ^2$

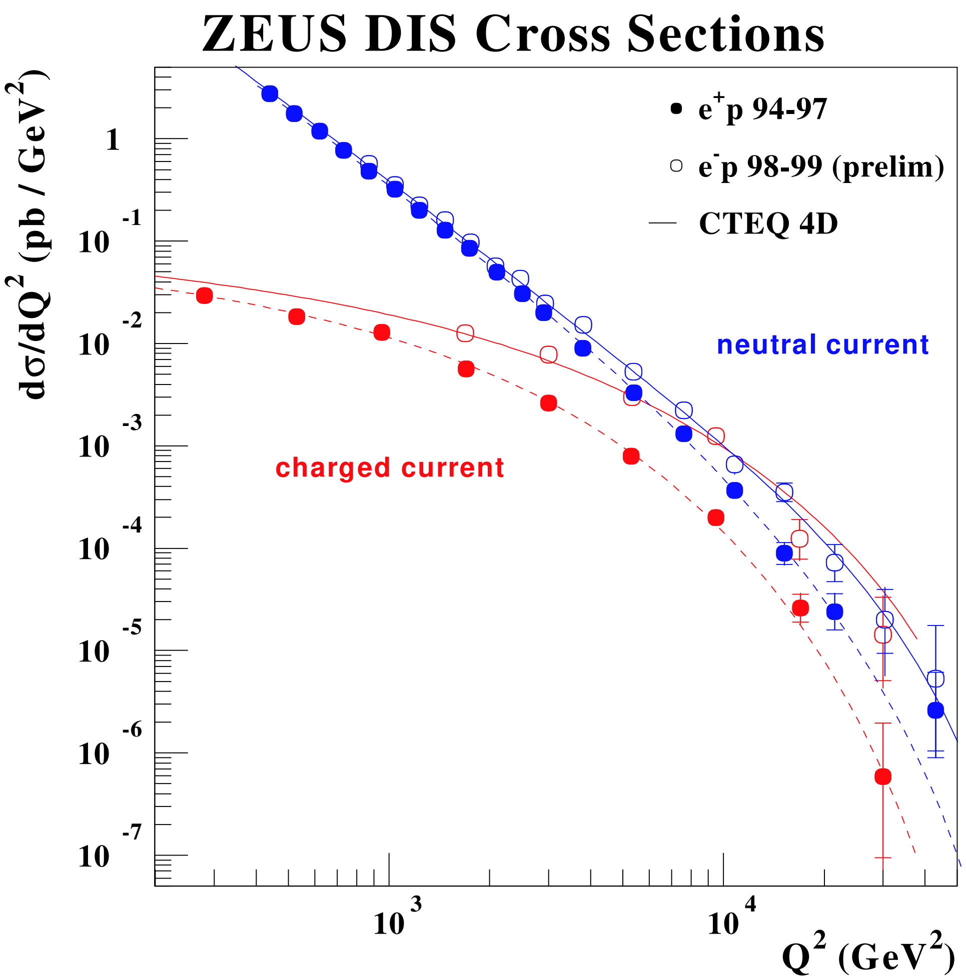

at large Q^2 neutral and charged current processes have cross sections of similar size

$\rightarrow$ electroweak unification

$$(G_F = \frac{\pi\alpha}{\sqrt{2}M_W^2}\frac{1}{(1-M_W^2/M_Z^2)})$$

differences due to
quark content and weak couplings of quarks

extraction of propagator mass

$$\sigma_{CC} \propto \frac{M_W^2}{M_W^2+Q^2}$$

Measurement of Propagator Mass

$$\frac{d\sigma}{dQ^2} = \sigma^0 \left(\frac{M_{prop}^2}{M_{prop}^2 + Q^2} \right)^2 \Phi_W$$

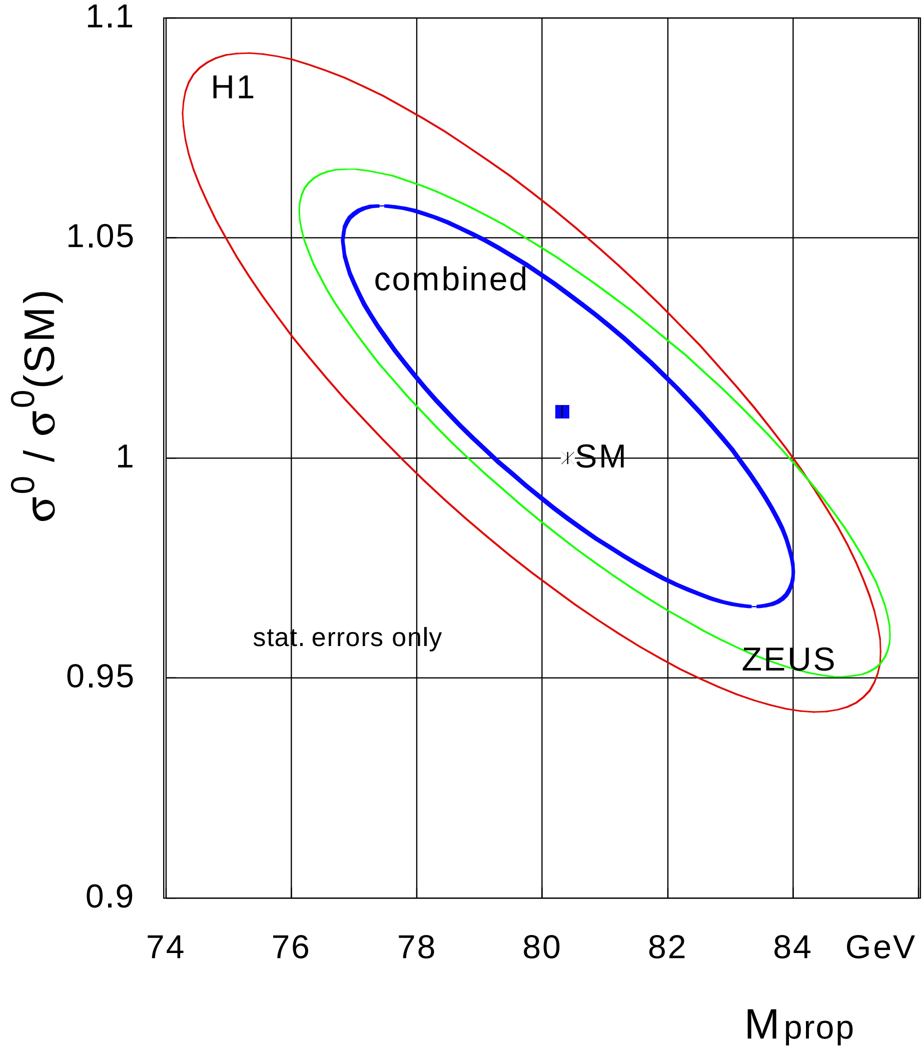

for fixed normalization (space-like regime)

$$M_{prop} = \begin{array}{ll} 80.9 \pm 3.3(stat.) \pm 1.7(syst.) \pm 3.7(pdf) GeV & \text{H1} \\ 81.4^{+2.7}_{-2.6}(stat.) \pm 2.0(syst.)^{+3.3}_{-3.0}(pdf) GeV & \text{ZEUS} \end{array}$$

world average: $M_W = 80.41 \pm 0.10$ GeV (time-like)

CC Cross Section and Parton Densities

Zeus: $e^+p : \mathcal{L} = 47.7pb^{-1}$

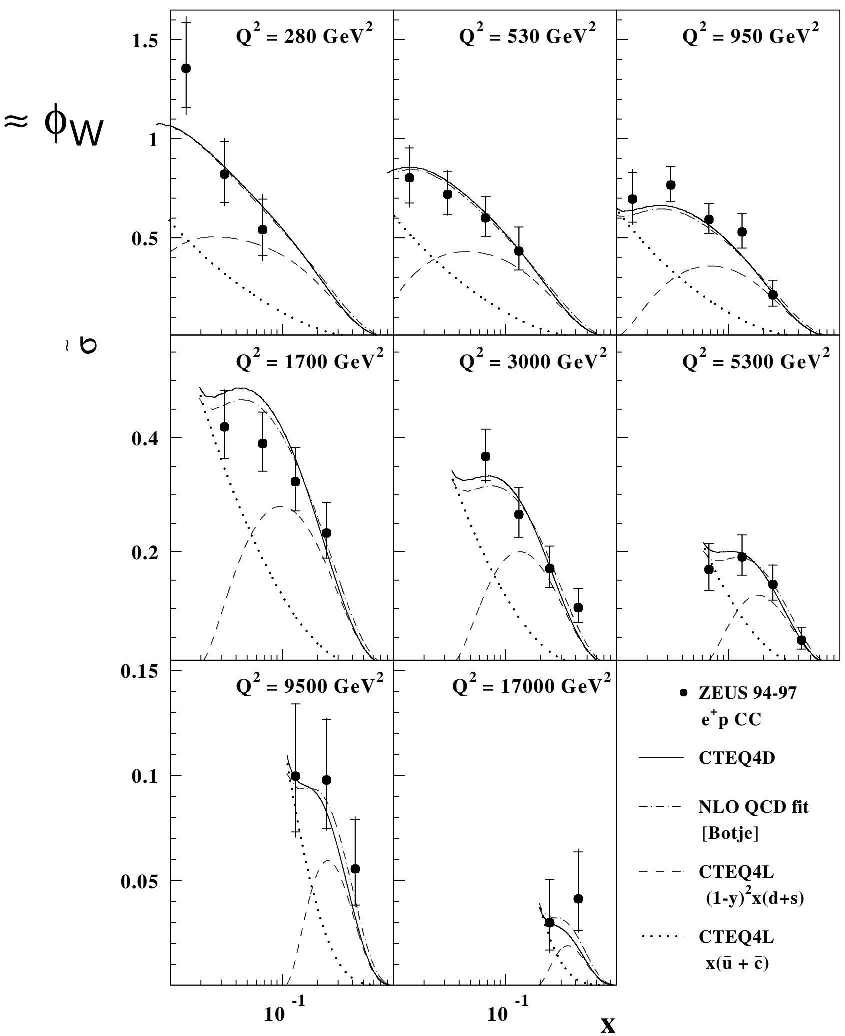

$$\frac{d^2\sigma_{CC}}{dx\, dQ^2} = \frac{G_F^2}{2\pi x}\left(\frac{{M_W}^2}{{M_W}^2+Q^2}\right)^2 \Phi_{CC}(x, Q^2)$$

$$\Phi_{CC}^{e^-p}|_{LO} = (u+c) + (1-y)^2(\bar{d}+\bar{s})$$

$$\Phi_{CC}^{e^+p}|_{LO} = (1-y)^2(d+s) + (\bar{u}+\bar{c})$$

cross section at high x

dominated by valence quarks

e^+: $\Phi \propto (1-y)^2 d$

rise towards low x

due to contribution of sea

CC Cross Sections in e^+p and e^-p

$e^+p : \mathcal{L} = 35 pb^{-1}$ $\quad$ $e^-p : \mathcal{L} = 15.3 pb^{-1}$

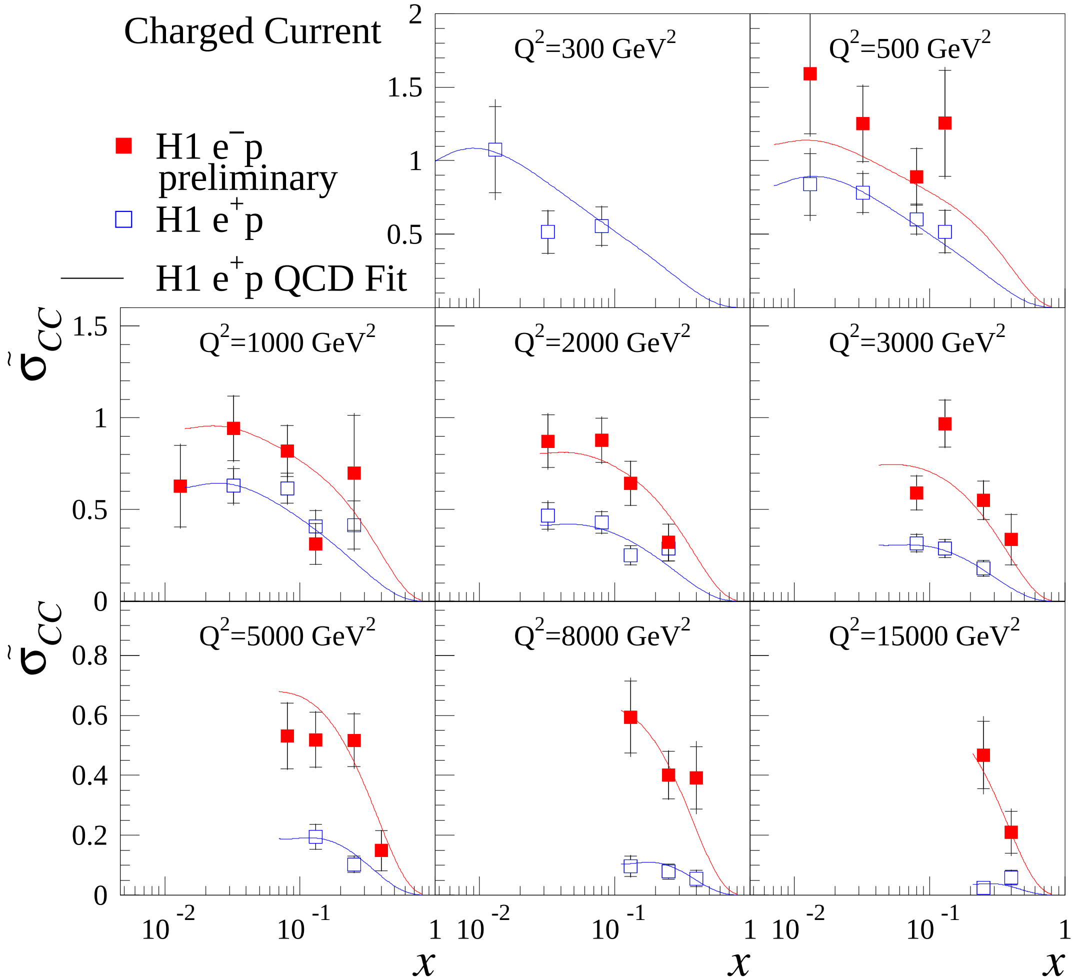

high Q^2, high x:
dominated by valence quarks
$\rightarrow$ order of magnitude difference

e^-: $\tilde{\sigma} \propto u$

e^+: $\tilde{\sigma} \propto (1-y)^2 d$

– $\dfrac{\int 1 dy}{\int (1-y)^2 dy} = 3$

– $u/d \gtrsim 2$

low Q^2, low x:
flavor symmetric sea
$\rightarrow$ decreasing difference

Conclusions

- Deep inelastic inclusive single and double differential cross sections are measured at HERA:
  $\frac{d\sigma^{e^-p}_{NC,CC}}{dQ^2}$, $\frac{d\sigma^{e^-p}_{NC,CC}}{dx}$, $\frac{d\sigma^{e^-p}_{NC,CC}}{dxdQ^2}$
  $\frac{d\sigma^{e^+p}_{NC,CC}}{dQ^2}$, $\frac{d\sigma^{e^+p}_{NC,CC}}{dx}$, $\frac{d\sigma^{e^+p}_{NC,CC}}{dxdQ^2}$
- description of data by the evolution of parton distributions works well up to the highest Q^2 values
  $\rightarrow$ test of pQCD
- γZ interference observed by comparison of e^+p and e^-p cross sections
- propagator mass in space-like regime extracted from Q^2 dependence of $\frac{d\sigma^{e^+p}_{CC}}{dQ^2}$
  $\rightarrow$ consistent with "time-like" M_W
- data confirm predictions of the standard model in both its QCD and electroweak sectors